Metal-Anion Sorption by Chitosan Beads: Equilibrium and Kinetic Studies

Guibal Eric, Céline Milot, John Michael Tobin

Metal-Anion Sorption by Chitosan Beads: Equilibrium and Kinetic Studies

Eric Guibal,*,† Céline Milot,† and John Michael Tobin‡

Laboratoire Génie de l'Environnement Industriel, Ecole des Mines d'Alès, 6 avenue de Clavières, 30319 Ales Cedex, France, and School of Biological Sciences, Dublin City University, Dublin 9, Ireland

Chitosan is a well-known biopolymer, whose high nitrogen content confers remarkable ability for the sorption of metal ions from dilute effluents. However, its sorption performance in both equilibrium and kinetic terms is controlled by diffusion processes. Gel bead formation allows an expansion of the polymer network, which improves access to the internal sorption sites and enhances diffusion mechanisms. Molybdate and vanadate recovery using glutaraldehyde cross-linked chitosan beads reaches uptake capacities as high as 7−8 mmol g^{-1}, depending on the pH. The optimum pH (3−3.5) corresponded to the predominance range of hydrolyzed polynuclear metal forms and optimum electrostatic attraction. While for beads, particle size does not influence equilibrium, for flakes, increasing sorbent radius significantly decreases uptake capacities to 1.5 mmol g^{-1}. Sorption kinetics are mainly controlled by intraparticle diffusion for beads, while for flakes the controlling mechanisms are both external and intraparticle diffusions. The gel conditioning increases the intraparticle diffusivity by 3 orders of magnitude: intraparticle diffusivities range between 10^{-13} and 10^{-10} m^2 min^{-1}, depending on the sorbent size and the conditioning.

Introduction

Recent developments in environmental quality standards highlight the need for improved wastewater treatment of dilute metal-bearing effluents. Biosorption, or sorption to material of biological origin, is recognized as an emerging technique for the depollution of heavy-metal polluted streams (Volesky and Holan, 1995). Several sorbents can be used: bacterial, algal (Volesky and Holan, 1995), or fungal biomass (Guibal et al., 1992) as well as biopolymers (Deans and Dixon, 1992). Chitosan is a biopolymer which is extracted from crustacean shells or from fungal biomass. The high proportion of amine functions in this natural polymer results in novel binding properties for metal ions such as cadmium, copper, lead, uranyl, mercury, and chromium (Eiden et al., 1980; Coughlin et al., 1990; Argüelles-Monal and Peniche-Covas, 1993). Modifying chitosan by organic acid grafting can improve sorption performances (Muzzarelli et al., 1985). The low porosity of native material introduces diffusion constraints which are rate-limiting (Findon et al., 1993). Intraparticle diffusion occurs in a restricted external layer of the particle for raw chitosan and in the whole mass of the sorbent for modified chitosan. Scanning electron microscopy allows this layer thickness to be estimated at approximately 40−50 μm for uranium sorption in raw chitosan (Guibal et al., 1995). These diffusion limitations result in a decrease of the sorption capacity of the polymer according to the volumetric ratio between usable and total volume of the particle. Similar results were observed with microcrystalline chitosan (Guibal et al., 1995).

* To whom all correspondence should be addressed. Tel.: +33 (0)4 66 78 27 34. Fax: +33 (0)4 66 78 27 01. E-mail: eguibal@ensm-ales.fr.

† Ecole des Mines d'Ales.

‡ Dublin City University.

An alternative protocol to improve the porosity of the chitosan has been proposed by several authors. Derived from a standard alginate bead formation procedure, it involves dissolution of chitosan flakes in an acetic acid solution followed by a precipitation in a dilute sodium hydroxide solution (Kawamura et al., 1993; Rorrer et al., 1993). Acid environments produce the partial dissolution of the polymer. Cross-linking of chitosan particles, in glutaraldehyde, epichlorhydrine, or EGDE (ethylene glycol glycidyl ether) enhances the resistance of sorbent beads against acid, alkali, or chemicals (Inoue et al., 1993; Rorrer et al., 1993).

As the above treatments are expected to modify equilibrium or kinetic behavior, the aim of this study focuses on the diffusion properties of porous chitosan chelating resins in order to correlate diffusion characteristics to chitosan conditioning. The structure of the chitosan polymer and its low "porosity" contribute to the low-metal-ion diffusivities. Diffusivities as low as 10^{-11}–10^{-14} m^2 s^{-1} are reported in several studies (Findon et al., 1993; Guibal et al., 1995). These values are 3−4 orders of magnitude lower than metal-ion diffusivities in pure water (Vanysek, 1993). The first part of this work is devoted to pH optimization. Other parameters are investigated in terms of both equilibrium and kinetic performances. Parameters investigated for their influence on metal-ion diffusion include metal-ion concentration, size of the beads, and agitation speed.

Materials and Methods

Materials. Chitosan was supplied by ABER-Technologie (France) as a flaked material, with a deacetylation percentage of approximately 87% (defined by IR spectrometry, Baxter et al., 1992). The mean molecular weight was measured at MW_m = 125 000 (using a size exclusion chromatography (SEC) method coupled with a differential refractometer and a multiangle laser light-scattering photometer, Piron et al., 1997). The pore size

Table 1. Physical Properties of Sorbent Particles

sorbent	d_p	ρ (g L^{-1})	experimental A/V[a] (m^2 m^{-3})	water content (%)	external surface[b] area (m^2 (wet) g^{-1})
flakes G1	0−125 μm	1180	15.90	13.0	81.4×10^{-3}
flakes G2	125−250 μm	1180	5.30	13.0	27.1×10^{-3}
flakes G3	250−500 μm	1180	2.66	13.2	13.6×10^{-3}
beads 1	0.95 mm	1021	17.77	93.2	7.11×10^{-3}
beads 2	1.6 mm	1023	10.19	93.8	3.72×10^{-3}
beads 3	2.8 mm	1021	6.085	94.3	2.04×10^{-3}

[a] The experimental A/V is calculated with a dry sorbent concentration of 170 mg L^{-1}. [b] The external surface area has been determined by the calculated ratio $6/d_p\rho$.

was difficult to measure by standard methods for gel beads in comparison with usual porous sorbents. The concept of pore diameter is not adequate and we will speak of the network opening as a general term. This network opening has been measured on cross-linked chitosan beads using the same analytical sytem (SEC) with high-molecular-weight dextran probes. The procedure indicated an opening size ranging from 14 to 30 nm. Glutaraldehyde is a Fluka AG product. Sodium hydroxide, ammonium molybdate, ammonium vanadate, and acetic and sulfuric acids were supplied by Prolabo.

Bead Formation Procedure. Milled chitosan flakes passed through a 250-μm sieve were dissolved in 4 w/w % acetic acid. The final weight percentage of chitosan was approximately 4 w/w %. The solution was allowed to stand for 7 days (the viscosity of chitosan solution decreased sharply with the time in the first days and then decreased more slowly). The solution was then pumped dropwise into a casting solution of sodium hydroxide (2.5 M) through a hypodermic nozzle (diameter of the nozzle, 0.6 mm; diameter of annular space of the apparatus around the nozzle, 3 mm). Depending on the diameter of the beads to be manufactured, air was blown through the annular space of apparatus with an increasing flow rate. Three bead diameters were studied: 0.95, 1.6, and 2.8 mm. The formed beads were allowed to stand in the precipitation bath for 16 h and then were washed and rinsed with demineralized water several times to a constant pH.

Chitosan Cross-Linking. Chemical cross-linking of chitosan chains with the bifunctional reagent glutaraldehyde occurs by a Schiff's reaction of aldehyde groups on glutaraldehyde with amine groups on the chitosan biopolymer chain (Roberts, 1992). The cross-linking bath contained a 2.5 wt % glutaraldehyde solution. The ratio of glutaraldehyde to chitosan beads was approximately 15 cm^3 g^{-1} of wet beads. Cross-linking occurred for 16 h. The cross-linked chitosan beads were extensively rinsed with demineralized water. Similar procedures were applied to manufactured cross-linked chitosan flakes at three particle sizes: G1 < 125 μm < G2 < 250 μm < G3 < 500 μm. Physical properties of the products are presented in Table 1. Dissolution testing in sulfuric acid solutions (pH ca. 3) has shown that chitosan does not significantly dissolve after the cross-linking step: chitosan concentration in the solution was measured using the acid red titration method (Gummow and Roberts, 1985). These findings demonstrate that the cross-linking is stable in our experimental conditions.

Experimental Procedure: Metal-Ion Adsorption. Ammonium molybdate (or vanadate) salts were used. Sorption isotherms were determined by contact of 200 mL of molybdate, or vanadate, solutions (of varying initial metal-ion concentrations: ca. 50, 100, and 200 mg L^{-1}) with known weights of wet cross-linked chitosan beads or cross-linked chitosan flakes (dry sorbent masses varying between 20 and 200 mg). All experiments were performed at room temperature and with a constant pH control, achieved by adding microvolumes of molar sodium hydroxide or sulfuric acid solutions. Samples were collected and separated (filtration through a 1.2-μm pore glass fiber membrane) after 72 h of agitation on an adjustable reciprocating shaker (150 rpm). The metal-ion content was determined by ICP spectrometry. The metal-ion content, q (mg g^{-1}), in the solid was determined by a mass balance (between solid and liquid phases). In this paper, all metal concentrations in both solid and liquid media are expressed as total metal (mg), to be independent of the form of the metal ion (free molybdate or vanadate, hydrolyzed species, etc.), while the sorbate is called the molybdate or vanadate ion as a general term. Kinetic studies were performed by mixing cross-linked chitosan wet beads or cross-linked flakes (equivalent dry mass of 170 mg) with 1 L of metal-anion solution. Agitation was provided at two agitator speeds (150 and 260 rpm). Samples were collected over time, filtered, and analyzed as described previously.

Sorption Kinetic Modeling. The sorption rate is known to be controlled by several factors including the following processes (Findon et al., 1993; Weber and DiGiano, 1996): (i) diffusion of the solute from the solution to the film surrounding the particle, (ii) diffusion from the film to the particle surface (external diffusion), (iii) diffusion from the surface to the internal sites (surface diffusion or pore diffusion), and (iv) uptake which can involve several mechanisms: physicochemical sorption, ion exchange, precipitation, or complexation. Bulk diffusion (i) is nonlimiting when agitation is sufficient to avoid concentration gradients in solution. Sorption is seen as a quasi-instantaneous mechanism. External mass-transfer resistance (ii) and intraparticle mass-transfer resistance (iii) are likely to be rate-controlling. Ficks' laws may be applied to describe mass-transfer rates.

External Diffusion. Mass transfer is governed by several relationships, taking into account the diffusion mechanisms and their related equations, the coupling between liquid and solid phases, and the initial and boundary conditions. The solution generally requires a numerical analysis. However, at early times of contact (between 0 and 15−20 min of contact) the system can be simplified by assuming that the concentration at the sorbent surface tends toward zero (pure external diffusion) and the intraparticle to be negligible. Thus, for external diffusion, the solution is given by

$$\ln \frac{C(t)}{C_0} = -k_f \frac{A}{V} t \qquad (1)$$

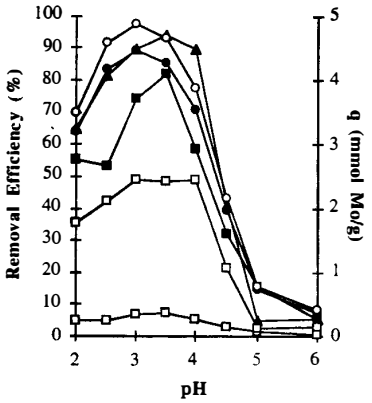

Figure 1. Influence of pH on molybdate sorption with varying initial molybdate concentrations (■/□, 8.8; ▲/△, 52; ●/○, 107 mg L^{-1}) for cross-linked chitosan beads (filled symbols, efficiency; open symbols, uptake capacity (mmol of Mo g^{-1})).

By plotting ln $C(t)/C_0$ against t (min), the initial external mass-transfer coefficient, k_f (m min^{-1}) may be determined ($C(t)$ is the solution concentration, C_0 the initial sorbate concentration (mg L^{-1}), A the sorbent exchange surface (m^2) and V the volume of solution (L)).

Intraparticle Diffusion I. McKay and Poots (1980) observed that the fraction of solute adsorbed can be expressed in terms of the square root of time. A plot of fraction of solute adsorbed against $t^{0.5}$ may be used to estimate the intraparticle diffusion rate in the linear range. This mathematical dependence of concentration in the solid on $t^{0.5}$ has been deduced by considering the sorption mechanism to be controlled by diffusion in the sorbent (as spherical particles) and by convective diffusion in the solution. The solution of the diffusion equations leads to a relationship between the concentration in the solid and the parameter $(Dt/a^2)^{0.5}$. Since D and a are considered constant during the experiment, the concentration varies as a function of $t^{0.5}$ as given by eq 2:

$$q(t) = x_i + k'\sqrt{t} \tag{2}$$

The slope of the linear part of the curve (uptake capacity vs square root time) gives the initial rate of sorption (here taken between 10 and 30–90 min), controlled by intraparticle diffusion, k' (mg g^{-1} $min^{-0.5}$) (McKay and Poots, 1980). The initial curve portion of the plot is attributed to boundary layer diffusion effects (i.e., external film resistance). The extrapolation of the linear straight lines to the time axis gives intercepts x_i, which are proportional to the boundary layer thickness.

Intraparticle Diffusion II. Crank (1975) proposed a model whereby diffusion is controlled only by intraparticle mass transfer for a well-stirred solution of limited volume (V), assuming the solute concentration always being uniform (initially C_0) and the sorbent sphere to be free from solute. Under these conditions, the total amount of solute M_t (mg g^{-1}) in a spherical particle after time t, expressed as a fraction of the corresponding quantity after infinite time (M_∞, mg g^{-1}) is given by

$$\frac{M_t}{M_\infty} = 1 - \sum_{n=1}^{\infty} \frac{6\alpha(\alpha+1)\exp(-Dq_n^2 t/d^2)}{9 + 9\alpha + q_n^2\alpha^2} \tag{3}$$

where D is the intraparticle diffusion coefficient (m^2 min^{-1}) and d is the particle diameter (m). The fractional approach to equilibrium, FATE, may be used to estimate the intraparticle diffusion coefficient D, when the external diffusion coefficient is being neglected. α is the effective volume ratio, expressed as a function of the equilibrium partition coefficient (solid/liquid concentrations ratio) and is obtained by the ratio $C_\infty/(C_0 - C_\infty)$. q_n represent the nonzero solutions of equations:

$$\tan q_n = \frac{3q_n}{3 + \alpha q_n^2} \quad \text{and} \quad \frac{M_t}{VC_0} = \frac{1}{1+\alpha} \tag{4}$$

The infinite sum terms are summed until the summation does not vary. In this study, eq 3 was used to determine the overall intraparticle diffusivity which best fitted the experimental data (minimizing the sum of the square of the differences between experimental results and calculated data).

Results and Discussion

pH Optimization. Prior to the sorption isotherm studies, the optimum pH for metal-ion uptake was determined. Figure 1 represents the molybdenum removal efficiency at equilibrium for varying pH, with initial metal concentrations of 8.8, 52, and 107 mg L^{-1}. It appears that the optimum pH is in the range 3–4. Similar observations have been cited by Inoue et al. (1993). The uptake capacity decreases about 25% at pH 2, while at pH 5 or 6, molybdate is not adsorbed. A slight shift appears with an increase of the molybdate concentration. At high concentration, the optimum pH is at 3, while at a lower concentration optimum pH is approximately 3.5. These results are generally consistent with previous observations on molybdate sorption by fungal biomass for which metal-anion binding was attributed to interaction with functional groups protonated at lower pH values (Tobin et al., 1984). The solubility increases above pH 1.5 and is not expected to affect sorption processes above pH 2.

In acid solution, with a pH significantly lower than the pK_a of chitosan, the nitrogen-containing functional groups (amines in free or substituted forms) of the biosorbent are protonated and the positive charge would be expected to attract anions. At near-neutral pH, the electrostatic balance between anionic and cationic groups on the polymer would be expected to be less favorable for molybdate binding.

The distribution of metal-ion species is also an important parameter in the interpretation of the pH effect on sorption performances. Figure 2 shows the distribution of molybdate species at both total molybdate concentrations 10 and 100 mg L^{-1}, from thermodynamic data presented by Baes and Mesmer (1976) and calculations performed with the program HYDRAQL (Papelis et al., 1988). At pH 3, the major species, which represents up to half of the total concentration, is $Mo_7O_{23}(OH)^{5-}$. At low concentrations, mononuclear and polynuclear hydrolyzed species coexist, while at high molybdate levels, molybdate occurs solely in condensed form. This distribution may influence metal uptake so that the optimum pH then depends on the total concentration. The fact that the optimum pH range varies slightly with the concentration may be related to the predominance of particular hydrolyzed species which are more favorable for sorption on pro-

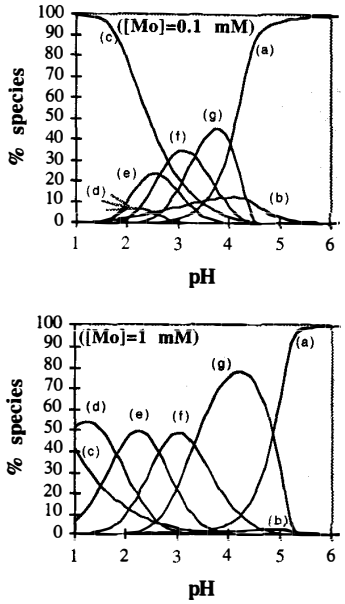

Figure 2. Molybdate chemistry: distribution of molybdate species as a function of pH and total molybdate concentration 0.1 and 1 mM (symbols correspond to (a) MoO_4^{2-}, (b) $HMoO_4^-$, (c) H_2MoO_4, (d) $Mo_7O_{21}(OH)_3^{3-}$, (e) $Mo_7O_{22}(OH)_2^{4-}$, (f) $Mo_7O_{23}(OH)^{5-}$, (g) $Mo_7O_{24}^{6-}$; the form $Mo_{19}O_{59}^{4-}$ existing in high-concentration solutions, at pH lower than 1.5, has been omitted).

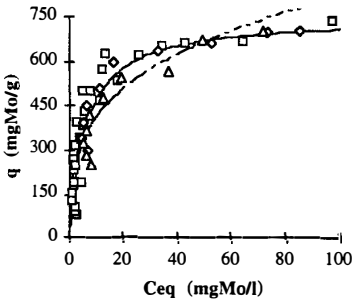

Figure 3. Molybdate sorption isotherms at pH 3. Experimental data and modeled curves (solid line: Langmuir model; dashed line, Freundlich model) for several bead sizes (B1, 0.95 mm, □; B2, 1.6 mm, ◇; B3, 2.8 mm, △).

tonated amine sites. At low initial concentration $Mo_7O_{24}^{6-}$ predominates at pH 3.5, while at higher initial concentration, at pH 3, $Mo_7O_{23}(OH)^{5-}$ is the predominant species. Both are strongly anionic species, which is consistent with the high-sorption levels observed. However, as no major differences in speciation over the pH range 3–4 are observed at the different metal concentrations, it is not possible to identify the cause of the variation in optimum pH for sorption. Inoue et al. (1993) indicate that the reduction in molybdate sorption, in a less acid medium, results from the formation and predominance of nonadsorptive anionic species, such as $HMoO_4^-$ and MoO_4^{2-}, a phenomenon commonly cited in the solvent extraction of Mo(VI) with acidic extractants.

Effect of Conditioning and Particle Size on Sorption Isotherms. *Beads Size.* Figure 3 shows the molybdate sorption isotherm at pH 3 for several bead sizes. The influence of bead size on sorption isotherms was investigated through covariance analysis. Computing the ANOCOV table (co-variance analysis) confirms that sorption capacity is independent of the bead sizes (the Fisher–Snedecor coefficient relative to the corresponding table is lower than the critical value with a 95% probability yield). These calculations were first performed on the cumulative data for beads of 0.95-mm diameter versus the data at other diameters. In contrast, Jha et al. (1988) report that cadmium sorption capacity drastically increases with a lowering of the chitosan sorbent size, indicating that metal-ion accumulation occurs by a surface mechanism. McKay et al. (1989) observed that sorption behavior varies for different metal ions: the separation factor was found to be independent of the particle size for mercury, but varied slightly with the particle size for copper, nickel, and zinc. Uranium sorption by chitosan and glutamate glucan have previously shown contrasting behavior: equilibrium uptake is independent of the particle size (and external surface) for substituted chitosan while chitosan adsorbs uranyl solely at its surface (Guibal et al., 1995).

Experimental data were further compared to the Langmuir and Freundlich sorption isotherm models (Figure 3). The Langmuir and Freundlich models are commonly used to fit experimental data when solute uptake occurs by a monolayer sorption. The Langmuir model assumes the surface of the sorbent to be homogeneous and the sorption energies to be equivalent for each sorption site. Solute immobilization occurs without mutual interactions between the molecules sorbed on the surface. The Freundlich model is based on an exponential distribution of sorption sites and energies. Moreover, molecules adsorbed on the surface can interact. Several other equations and models exist to describe such equilibrium conditions. The Temkin and Dubinin–Radushkevich models are more general than those of Langmuir and Freundlich (Nestle and Kimmich, 1996). They do not not assume an energetically homogeneous surface and propose a nonhomogeneous distribution of sorption sites. In particular, the Dubinin–Radushkevich model assumes that ionic species bind first with the most energetically favorable sites and that multilayer adsorption then occurs. These models were tested in the present work (data not shown) but did not exhibit good fit to the sorption data. It appears that the Langmuir model best fits the experimental results over the experimental range (Tables 2 and 3). Gel formation expands the structure of the chitosan network. Consequently, interactions which may occur in raw chitosan between neighboring sites are less likely. The absence of transmigration of sorbate in the plane of the surface may explain the good fit observed with the Langmuir model.

A statistical study (ANOCOV table) on beads, of diameter 0.95 mm, shows that varying the initial concentration (27, 56.5, and 100 mg of Mo L^{-1}) leads to a Fisher–Snedecor coefficient rather higher than the limiting coefficient at a probability yield of 95%. This confirms that the sorption level is dependent on the initial concentration: metal speciation and high hydrated metal-ion radius control steric hindrance and access to internal sites.

Conditioning of Chitosan. Molybdate sorption isotherms for several flake particle sizes, compared to those of beads, are shown in Figure 4a. While the maximum uptake varies little between G2 and G3 classes, it increases considerably for the smallest particles G1.

Table 2. Sorption Isotherm Constants for Molybdate Uptake at pH 3[a]

experimental runs		Langmuir model			Freundlich model		
type	size	q_m (mg g^{-1})	b (L mg^{-1})	MSR[b]	k_F (g^{-1} $L^{1/n}$ $mg^{1-1/n}$)	n	MSR[b]
B1	0.95 mm	763.0 (7.95)	0.177 (17.01)	78.6	201.3 (8.82)	3.18	98.9
B2	1.6 mm	747.9 (7.80)	0.179 (17.25)	40.5	271.3 (7.90)	4.44	63.2
B3	2.8 mm	761.7 (7.94)	0.121 (11.62)	52.3	197.0 (8.29)	3.27	93.4
beads	Cumul	748.8 (7.80)	0.169 (16.22)	72.7	211.3 (8.42)	3.40	87.4
G1	0–125 μm	329.7 (3.44)	0.550 (13.42)	20.4	165.7 (3.52)	6.40	27.0
G2	125–250 μm	193.9 (2.02)	0.595 (57.11)	11.3	124.5 (2.07)	9.82	10.4
G3	250–500 μm	184.5 (1.92)	0.140 (52.78)	12.2	62.7 (1.82)	4.45	9.4

[a] B, beads; F, flakes; size, diameter or class size; numbers into brackets represent molar determination of parameters instead of massic representation: q_m (mmol g^{-1}), b (L $mmol^{-1}$), k_F ($L^{1/n}$ g^{-1} $mmol^{1-1/n}$)). [b] MSR = mean square deviation calculated as:

$$\left[\frac{\sum_{i=1}^{n}[(X_{exp,i} - X_{cal,i})^2]}{n}\right]^{1/2}$$

Table 3. Sorption Isotherms Constants for Vanadate Uptake at pH 3[a]

experimental runs		Langmuir model			Freundlich model		
type	size	q_m (mg g^{-1})	b (L mg^{-1})	MSR	k_F ($g^{-1}L^{1/n}$ $mg^{1-1/n}$)	n	MSR
B1	0.95 mm	402.5 (7.9)	0.24 (11.98)	40.1	196.5 (7.2)	6.28	40.5
G1	0–125 μm	250.4 (4.9)	0.22 (11.36)	26.2	95.5 (4.4)	4.60	37.3
G2	125–250 μm	165.2 (3.2)	0.80 (40.65)	5	121.2 (3.1)	14.17	5.5
G3	250–500 μm	146.8 (2.9)	0.21 (10.97)	12.3	58.9 (2.6)	4.86	14.6

[a] Numbers into brackets represent molar values: q_m (mmol g^{-1}), b (L $mmol^{-1}$), k_F ($L^{1/n}$ g^{-1} $mmol^{1-1/n}$)).

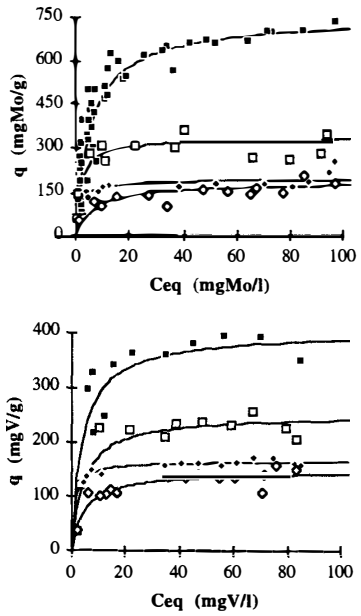

Figure 4. Conditioning effect on (a) molybdate and (b) vanadate sorption isotherms. (Curves, Langmuir model; beads: B1, 0.95 mm; B2, 1.6 mm; B3, 2.8 mm. Flakes: G1, 0–125 μm; G2, 125–250 μm; G3, 250–500 μm.)

This trend has also been observed for uranium removal by a chitosan sorbent (Guibal et al., 1995). It appears that metal-ion removal is controlled by surface sorption or by sorption/diffusion restricted to an external thin layer. The maximum uptake of chitosan flakes does not exceed half that obtained with chitosan beads: approximately 3.5 mM g^{-1} (350–400 mg g^{-1}) compared to 7 mM g^{-1} (about 700–750 mg g^{-1}). A similar trend is observed for vanadate removal by chitosan flakes (Figure 4b). However the difference between flake and bead maximum sorption levels is less than that for molybdate: 2.9 mM g^{-1} compared to 4.2 mM g^{-1} (150 and 400 mg g^{-1}, respectively).

These results confirm the strong influence of the conditioning and of the expansion of the diffusion network on the sorption capacity of chitosan-based sorbents. Rorrer et al. (1993) have reported similar findings and proposed a pore blockage model. They suggested that the variation in sorption capacity was not due to exchange surface area, but that it was related to the formation of adsorbed metal clusters which may constrict or completely block pores. Tables 2 and 3 summarize the Langmuir and the Freundlich model parameters for varying experimental conditions (conditioning forms and particle sizes) for molybdate and vanadate, respectively.

Sorption Kinetics: Influence of Experimental Parameters. *Agitator Speed.* Two agitator speeds were used in these studies: 150 and 260 rpm (initial molybdate concentration 100 mg L^{-1}, pH 3, chitosan bead diameter 0.95 mm, and dry sorbent concentration 170 mg L^{-1}). The variation in agitator speed was restricted to these values to avoid mechanical degradation of the bead structure. The differences observed on rate parameters are not appreciable: the film mass-transfer coefficients decreased from 10.1×10^{-4} to 8.9×10^{-4} m min^{-1}, while the intraparticle diffusivity is decreased from 6.3×10^{-11} to 5.9×10^{-11} m^2 min^{-1}. The intraparticle diffusion coefficient (k') varies by less than 3% and the boundary layer thickness parameter ($\sqrt{t_{lim}}$) is almost unchanged. These results confirm the non-limiting influence of external diffusion in the overall sorption process in the speed range investigated. It is well-known that the sorption rate is controlled by the agitation speed for systems controlled by external diffusion (Hellferich, 1995). Increasing the agitation speed increases turbulence in the solution, which in turn reduces the thickness of the external boundary layer. Similar trends have been observed on uranium sorption by glutamate glucan and NDTC (*N*-[2-(1,2-dihydroxyethyl)tetrahydrofuryl]chitosan: a chitosan-based poly-

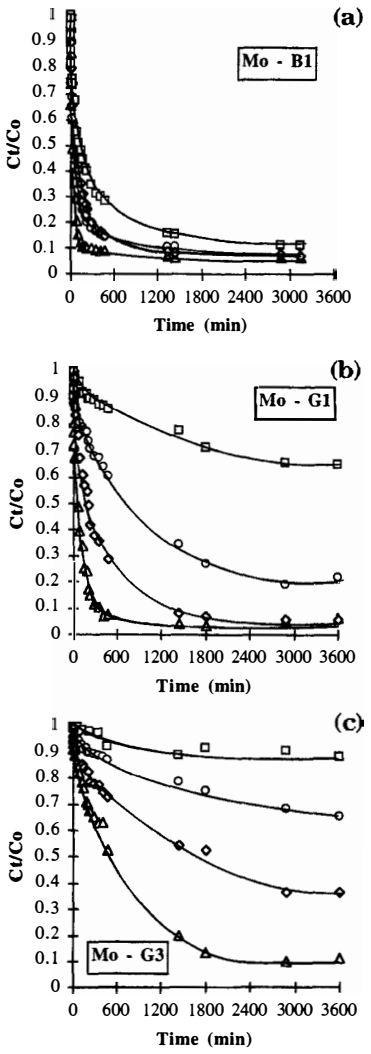

Figure 5. Effect of initial concentration on molybdate sorption ((a) B1 beads (diameter 0.95 mm), (b) G1 flakes (0–125 μm), (c) G3 (250–500 μm); agitation speed, 150 rpm; dry sorbent concentration, 170 mg L^{-1}). The symbols △, ◇, ○, and □ represent respectively the following: (Mo-B1) 12, 28, 54, and 108; (Mo-G1) 10, 26, 54, and 107; (Mo-G3) 10, 27, 51, and 107.

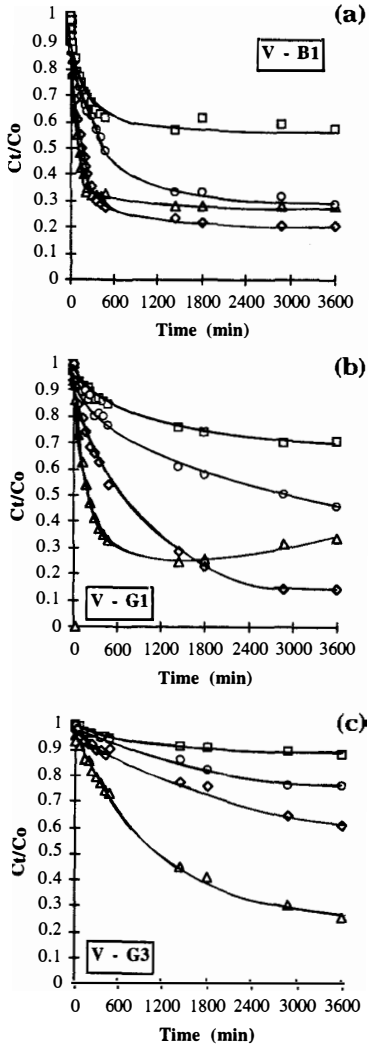

Figure 6. Effect of initial concentration on vanadate sorption ((a) B1 beads (diameter 0.95 mm), (b) G1 flakes (0–125 μm), (c) G3 (250–500 μm); agitation speed, 150 rpm; dry sorbent concentration, 170 mg L^{-1}). The symbols △, ◇, ○, and □ represent respectively the following: (V-B1) 10, 25, 47, and 87; (V-G1) 9, 24, 46, and 91; (V-G3) 9, 23, 46, and 91.

mer obtained by ascorbic acid substitution on chitosan) (Guibal et al., 1995). Findon et al. (1993) also reported copper and mercury sorption to chitosan to be independent of the agitation speed.

Metal-Anion Concentration. Molybdate and vanadate sorption kinetics for varying initial concentrations for flakes G1 and G3 and beads B1 particles are shown in Figures 5 and 6, respectively. Diffusion coefficients are summarized in Table 4 (for molybdate) and Table 5 (for vanadate). It can be seen that k_f varies inversely with C_0. Regression analysis shows that k_f varies as a power of the initial molybdate concentration for sorbent beads according to the following equation:

$$k_f = (3.382 \times 10^{-3}) C_0^{0.291} \quad (R^2 = 0.979) \qquad (5)$$

This effect is considerably more marked in the flake studies where k_f decreases by over an order of magnitude with increasing initial concentration for each particle size. Therefore, it appears that external diffusion contributes to the control of the sorption rate, principally for flakes. This influence is likely related to the varying distribution of molybdate species with increasing concentrations.

Increasing the initial concentration reduces the contribution of the external film resistance (column 4, Table 4). The lower the $\sqrt{t_{\text{lim}}}$, the thinner the external boundary layer. At all present molybdate concentrations, the value of $\sqrt{t_{\text{lim}}}$ is lower than 1. Under these conditions, the layer is very thin. However, for G3 flakes, the calculation of the intraparticle mass-transfer coefficients of both molybdate and vanadate by the McKay procedure gives negative values for the axis intercept. This would appear to indicate that no single controlling-mechanism model can be applied to accurately describe the sorption mass transfer for chitosan

Table 4. Effect of the Molybdate Concentration, Type, and Size of Sorbent on the Sorption Rate and Diffusion Coefficients[a]

C_0 (mg L^{-1})	sorbent type/size	$k_f \times 10^4$ (m min^{-1})	$\sqrt{t_{lim}}$ ($min^{0.5}$)	k' (mg g^{-1} $min^{-0.5}$)	D (m^2 min^{-1})
12	B1	19.5	0.75	8.2	1.4×10^{-10}
28	B1	13.9	0.48	14.4	1.2×10^{-10}
53	B1	12.4	0.13	21.2	5.9×10^{-11}
108	B1	10.1	0.14	33.8	5.2×10^{-11}
108	B2	10.9	0.71	25.3	7.4×10^{-11}
108	B3	5.9	0.96	16.1	1.6×10^{-11}
10.5	G1	12.2	0.01	3.8	1.8×10^{-13}
26.0	G1	4.8	NS	5.6	7.2×10^{-14}
54.2	G1	3.9	0.05	4.8	8.6×10^{-14}
107.3	G1	1.0	0.04	3.9	1.6×10^{-13}
107.3	G2	0.55	0.003	1.2	1.2×10^{-12}
10.3	G3	29.6	0.02	1.2	6.3×10^{-12}
27.3	G3	3.8	NS	NS	4.8×10^{-12}
50.8	G3	2.3	NS	2.2	3.6×10^{-12}
106.6	G3	0.25	NS	0.8	1.7×10^{-12}

[a] Beads: B1, 0.95 mm; B2, 1.6 mm; B3, 2.8 mm. Flakes: G1 < 125 μm < G2 < 250 μm < G3 < 500 μm. NS: nonsignificant.

Table 5. Effect of the Vanadate Concentration, Type, and Size of Sorbent on the Sorption Rate and Diffusion Coefficients[a]

C_0 (mg L^{-1})	sorbent type/size	$k_f \times 10^4$ (m min^{-1})	$\sqrt{t_{lim}}$ ($min^{0.5}$)	k' (mg g^{-1} $min^{-0.5}$)	D (m^2 min^{-1})
10	B1	7.0	NS	3.0	2.1×10^{-10}
25	B1	4.7	0.02	2.5	1.0×10^{-10}
47	B1	2.4	NS	1.5	5.4×10^{-11}
87	B1	2.0	NS	1.3	2.0×10^{-10}
47	B2	6.0	0.016	1.3	1.4×10^{-10}
47	B3	6.7	0.011	0.8	2.6×10^{-10}
9.0	G1	4.4	0.003	1.7	4.2×10^{-13}
23.7	G1	0.9	0.01	2.6	7.3×10^{-14}
46.1	G1	1.3	NS	2.7	1.2×10^{-13}
90.9	G1	0.3	0.008	3.6	2.4×10^{-13}
46.0	G2	2.8	0.008	1.2	1.6×10^{-12}
9.0	G3	29.1	0.01	0.6	2.6×10^{-12}
22.7	G3	2.6	0.003	0.8	3.7×10^{-12}
45.8	G3	1.6	NS	0.9	4.6×10^{-12}
90.6	G3	0.55	NS	1.5	8.3×10^{-12}

[a] Beads: B1, 0.95 mm; B2, 1.6 mm; B3, 2.8 mm. Flakes: G1 < 125 μm < G2 < 250 μm < G3 < 500 μm.

flakes. A mixed external and intraparticle diffusion model would likely be required.

Similarly, regression analysis shows that the variation of the initial internal sorption rate with the concentration obeys the following relation for molybdate and beads:

$$k' = 1.657 C_0^{0.644} \qquad (R^2 = 0.999) \tag{6}$$

Some differences are observed between beads and flakes. The diffusivity of molybdate into chitosan beads decreases slightly with a 9-fold increase of the initial concentration (order of magnitude: 10^{-10} m^2 min^{-1}). For G3 flakes the intraparticle diffusivity slightly increases (around 5×10^{-12} m^2 min^{-1}) with increasing initial concentration, while for G1 flakes the variation is not continuous (order of magnitude: 10^{-13} m^2 min^{-1}). Moreover, diffusivity into chitosan beads is seen to reach a value lower (approximately 2 orders of magnitude lower) than the molecular diffusivity in water (Vanysek, 1993), while for G1 flakes this difference can reach about 5 orders of magnitude.

As shown in Table 5, vanadate sorption exhibites a similar trend: the variations are not very marked with increasing initial concentration. The diffusivity magnitude is of the same order for both molybdate and vanadate ions. Comparing experiments performed at the same initial molar concentrations, it is interesting to note that, for low initial concentrations, the vanadate intraparticle diffusivity is frequently higher than that of molybdate and often in the ratio of 2:1, the reciprocal of the ratio of atomic masses of molybdenum and vanadium elements.

Variations in diffusivity may be explained by partial inadequacy of the present simple diffusion models to describe phenomena resulting from heterogeneities of the gel matrix and the possible occurrence of mixed absorption and adsorption mechanisms. Nestle and Kimmich (1996), in a study of copper diffusion in alginate gels, postulated a non-Fickian diffusion to explain the variation of the diffusion coefficient with the concentration. The high metal uptake capacities reached with those sorbents involved possible variations in the isosteric heat of adsorption, the surface diffusivity being a function of the surface coverage (as shown by Gilliland et al. (1974) for gases adsorption). Here, diffusivities in the solid decrease with the initial concentration (i.e., with the uptake capacity and the surface coverage). In contrast to the present work, Jang et al. (1990) obtained an increase in the copper diffusivity in alginate beads when the copper concentration was increased.

Beads or Flakes Sizes. Figure 5 shows the effect of the bead diameter on the sorption kinetics. Table 4 summarizes the diffusion coefficients obtained for molybdate sorption by several beads and flakes sizes. As expected, the sorption rate decreased with increasing sorbent particle size as the time required to reach equilibrium significantly increased. Table 4 shows that for studies at equal initial concentration (108 mg L^{-1}), k_f, the external mass-transfer coefficient decreased less than twice with increasing beads size, while the external boundary layer thickness slightly increased and the intraparticle mass-transfer coefficient k' slightly decreased. This k_f decrease has also been reported for uranium sorption by glutamate glucan (Guibal et al., 1995) and for copper sorption by raw chitosan. In contrast, mercury sorption to chitosan is not controlled by intraparticle diffusion (McKay et al., 1989). For flakes, the variations with particle size are nonappreciable. Mass transfer is controlled by both intraparticle and external resistance for flakes, the predominant control depending on the experimental conditions. For beads, the intraparticle mass transfer is enhanced by the gel formation and the external mass-transfer coefficient is less sensitive to particle size in comparison with nonporous flakes. Moreover, the external mass-transfer coefficients for beads are markedly greater than those for flakes. Gel expansion offers a greater external surface for a same dry mass and favors external mass transfer.

For molybdate sorption by cross-linked beads, regression analysis shows that the initial sorption rate obeyed the following relation:

$$k' = 0.286 d_p^{-0.689} \qquad (R^2 = 0.989) \tag{7}$$

The initial intraparticle mass-transfer rate does not vary with the reciprocal of the first power of the beads size. Morris and Weber (1962) have observed that the intraparticle mass-transfer rate (here denoted k') varied with the reciprocal of the first power of the sorbent particle diameter in two cases: when sorption occurs

on external sites of a nonporous adsorbent and when sorption was governed by external mass transfer on a porous adsorbent. Conversely, for intraparticle diffusion controlled sorption kinetics onto porous sorbents, the rate parameter varies with the reciprocal of some power of the diameter (Crank, 1975). Here, external resistance can be neglected for beads. For molybdate and beads, the variation in the intraparticule diffusion coefficient is not appreciable: the diffusivity varies between 10^{-11} and 8×10^{-11} m^2 min^{-1}, while for flakes the differences are greater (ranging from 7.2×10^{-14} to 6.3×10^{-12} m^2 min^{-1}).

Figure 6 shows the effect of the initial concentration for varying types and sizes of sorbent particles on vanadate sorption. While for molybdate ions the equilibrium C_t/C_0 sorption levels are equivalent for beads, for vanadium these values decrease with increasing concentration. In contrast, C_t/C_0 values increase with increasing initial concentration for both vanadate and molybdate sorption to chitosan flakes. Comparison of Figures 5 and 6 indicates that the sorption rate is more rapid for molybdate than that for vanadate. This is confirmed by a comparison of Tables 4 and 5 wherein all of the kinetic parameters are greater for molybdate than for vanadate, and these differences are especially pronounced for beads. Flakes exhibit similar behavior for vanadate and molybdate in terms of size effect: G1 and G2 particle sizes yield similar sorption curves, while G3's size differs significantly. The same orders in external mass-transfer coefficients k_f are obtained for molybdate and vanadate solutions. As expected, it appears that for both molybdate and vanadate solutions, intraparticle diffusivities are almost independent of particle size for beads but not for flaked particles. Such differences indicate that sorption kinetics are well-described by an intraparticle diffusion model for beads sorbents, while the model does not adequately represent flaked materials behavior. Analysis of diffusion mechanisms for flaked particles is problematic, and models cited previously cannot be easily applied to evaluate variations in rates and diffusivities with the particle size. Even if intraparticle diffusion is the controlling step, external mass transfer obeys the criteria described by Hellferich (1995) and its contribution to the diffusion control is increased for small particles of low-porous materials. However, this simplified approach is sufficient to give an evaluation of the parameter effect and to select which parameters control sorption kinetics.

Conclusion

Sorption of anions molybdate and vanadate shows similar behavior which is likely due to the similarities in the chemistry of these ions. A pH of approximately 3 is favorable for the sorption of these metal anions, which is consistent with (i) the electrostatic attraction between the protonated amine sites and the strongly anionic metal species and (ii) the appearance of polynuclear hydrolyzed metal species in the 3–3.5 pH range. Molar uptake capacity is similar for both molybdate and vanadate sorption in single-metal solution (7 mmol g^{-1} for both molybdate and vanadate removal onto chitosan gel beads). The sorption of molybdate and vanadate appears to be controlled mainly by the conditioning of the polymer. While sorption capacity is independent of the size of the chitosan gel beads, in the flaked forms the particle size drastically influences sorption performance. This observation suggests that the control of

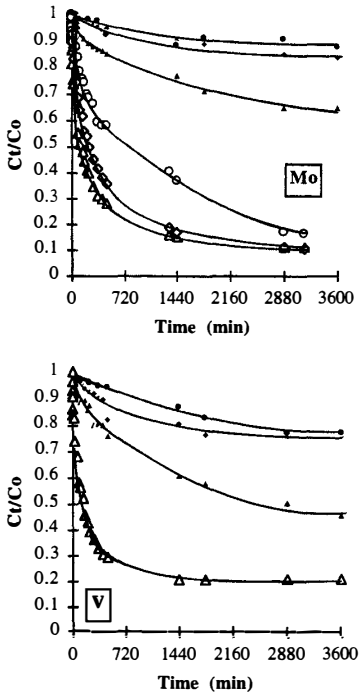

Figure 7. Effect of beads (open symbols) and flakes (filled symbols) size on molybdate (C_0, 108 mg L^{-1}) and vanadate (C_0, 50 mg L^{-1}) sorption (G1/B1, ▲/△; G2/B2, ◆/◇; G3/B3, ●/○; agitation speed, 150 rpm; dry sorbent concentration, 170 mg. L^{-1}).

the uptake results from surface limitations for flaked particles. These results can also be explained by a change in the rigidity of the polymer due to hydrogen bonding between chitosan chains. The dissolution/precipitation procedure favors the destruction of such bondings. However, a comparison of specific surface area, measured by BET analysis, for flaked and gelled sorbents (freeze-dried) shows a large increase with the gel conditioning (from 1 to 2 to 80–250 m^2 g^{-1}) and indicates that the expansion may represent the most significant cause for the enhancement of sorption properties.

In terms of kinetic behavior, metal-anion biosorption to chitosan gels is enhanced as compared to the native polymer (Figure 7). Diffusivities in the gel beads are of the range 10^{-10}–10^{-11} m^2 min^{-1} as compared to values of 10^{-12}–10^{-14} m^2 min^{-1} for the native polymer. Intraparticle diffusivities for gold and zinc cyanides onto anion-exchange resins of the same order $9–30 \times 10^{-11}$ m^2 min^{-1} were reported by Glover et al. (1990). Such values are lower than those presented by Chen et al. (1993) for the copper removal by alginate beads, at around 8×10^{-8} m^2 min^{-1}. For flaked sorbents, the decrease in diffusivities, as compared to those in water, is more evident, and this is particularly so for the smallest particle sizes. The reduction in size of the flaked particles offers a greater surface for exchange between solution and solid, favoring the external mass transfer. The resulting driving force between the solid and the solution is reduced.

The Biot number ($Bi = k_f d/D$) calculated from the ratio of the rate of external mass transfer to intraparticle mass transfer is significantly higher than 100, proving that overall diffusion and sorption are mainly

controlled by intraparticle diffusion. The modified Biot number ($Bi' = k_F d C_0 / D \rho q_0$), alternatively used to compare external and intraparticle mass resistance, gives with the present results values greater than 1 (Tien, 1994). The greater Bi', the more predominant intraparticle mass-transfer resistance. The external diffusion influence is much more marked for the lowest sorbent sizes.

Furthermore, these interpretations are complicated by the behavior of metal-anion species in solution. The hydrolysis of molybdate and vanadate changes their electrical conductivity, the size of their ionic and hydrated forms, and the corresponding diffusivity. The intraparticle diffusivities were dramatically reduced by 3 orders of magnitude for flakes. Rorrer et al. (1993) have presented findings which contrast to those of this paper: namely that small size beads (diameter: 1 mm) and powder chitosan exhibit similar cadmium sorption capacity and rates. These differences in the sorption behavior may be related to the size of hydrated ions: single cadmium ions in contrast to polynuclear molybdate or vanadate forms. Studies of membrane processes and diffusion have shown that diffusivities in membranes and solids are controlled by the ratio of the size of the solute to the size of the pore (Krajewska, 1995; Michard et al., 1996). Renkin (1954) established empirical relationships between the solid diffusivity/molecular diffusivity ratio and the molecule size/pore size ratio. This has been described by Papelis et al. (1995) for the adsorption of cadmium and selenite on micro- and mesoporous transition aluminas, by relating the ion diffusivities to their hydrated radii and to the pore size distribution of the materials. Tanaka et al. (1984) observed that diffusion in alginate beads was controlled by the molecular size of the substrate: for the smallest substrates the diffusivity was equivalent to those obtained in water, while for the largest substrates, no transfer was observed from the solution to the particle. The expansion of the structure of the polymer by the gel formation reduces the steric hindrance due to metal ions of large ionic or hydrated radii; with native material, the steric hindrance has less of an influence on the diffusion of small metal ions.

The interest of the modification of chitosan is not limited to the enhancement of diffusion properties. This modification may further obviate the high-pressure drop often observed with flaked chitosan in fixed-bed systems. The swelling and crumbling of raw chitosan introduces important dysfunctioning in packed columns which are usually employed in wastewater treatment. Cross-linked gel beads are presently used successfully for the treatment of industrial wastewaters containing molybdate at pilot scale.

The diffusion properties are greatly influenced by the structure of the polymer as has been shown previously for alginate materials. Several parameters influence the capacities of the polymer gel: the casting step (NaOH concentration), the cross-linking stage (nature and concentration of the cross-linking agent, hetero- and homogeneous cross-linking), the chitosan concentration in the bead (especially in the primary dissolution step), and also the intrinsic properties of the chitosan (deacetylation percentage and viscosity). Such parameters are now under investigation, with respect to sorption capacities, mechanical and chemical resistance, and diffusion properties.

Acknowledgment

Acknowledgments are due to the Ministère de l'Enseignement de la Recherche et de la Technologie (France) for the research fellowship of C. Milot. We would like to acknowledge Pr. Domard and his group (Dr. Zydowicz and Mr. Lucas), at the Laboratoire d'Etude des Matières Plastiques et des Biomatériaux, LEMPB (Université Claude Bernard Lyon I, France) for the determination of some physicochemical properties of the chitosan samples (deacetylation percentage, molecular weight, and distribution of network opening size).

Literature Cited

Argüelles-Monal, W.; Peniche-Covas, C. Preparation and characterization of a mercaptan derivative of chitosan for the removal of mercury from brines. *Angew. Makromol. Chem.* **1993**, *207*, 1–8.

Baes, C. F., Jr.; Mesmer, R. E. *The Hydrolysis of Cations*; John Wiley & Sons Inc.: New York, 1976.

Baxter, A.; Dillon, M.; Taylor, K. D. A.; Roberts, G. A. F. Improved method for IR determination of the degree of *N*-acetylation of chitosan. *Int. J. Biol. Macromol.* **1992**, *14*, 122–128.

Chen, D.; Lewandowski, Z.; Roe, F.; Surapaneni, P. Diffusivity of Cu^{2+} in calcium alginate gel beads. *Biotechnol. Bioeng.* **1993**, *41*, 755–760.

Coughlin, R. W.; Deshaies, M. R.; Davis, E. M. Chitosan in crab shell wastes purifies electroplating wastewater. *Environ. Prog.* **1990**, *9*, 35–39.

Crank, J. *The Mathematics of Diffusion*; Clarendon Press: Oxford, 1975.

Deans, J. R.; Dixon, B. G. Uptake of Pb^{2+} and Cu^{2+} by novel biopolymers. *Water Res.* **1992**, *26*, 469–472.

Eiden, C. A.; Jewell, C. A.; Wightman, J. P. Interaction of lead and chromium with chitin and chitosan. *J. Appl. Polym. Sci.* **1980**, *25*, 1587–1599.

Findon, A.; McKay, G.; Blair, H. S. Transport studies for the sorption of copper ions by chitosan. *J. Environ. Sci. Health* **1993**, *A28*, 173–185.

Gilliland, E. R.; Baddour, R. F.; Perkinson, G. P.; Sladek, K. J. Diffusion on surfaces. I. Effect of concentration on the diffusivity of physically adsorbed gases. *Ind. Eng. Chem. Fundam.* **1974**, *13*, 95–100.

Glover, M. R. L.; Young, B. D.; Bryson, A. W. Modelling the binary adsorption of gold and zinc cyanides onto a strong-base anion-exchange resin. *Int. J. Miner. Process.* **1990**, *30*, 217–228.

Guibal, E.; Roulph, C.; Le Cloirec, P. Uranium biosorption by a filamentous fungus *Mucor miehei*: pH effect on mechanisms and performances of uptake. *Water Res.* **1992**, *26*, 1139–1145.

Guibal, E.; Jansson-Charrier, M.; Saucedo, I.; Le Cloirec, P. Enhancement of metal ion sorption performances of chitosan: effect of the structure on the diffusion properties. *Langmuir* **1995**, *11*, 591–598.

Gummow, B. D.; Roberts, G. A. F. Studies on chitosan-induced metachromasy, 1. Metachromatic behaviour of sodium 2′-hydroxy-1, 1′-azo-naphthalene-4-sulfonate in the presence of chitosan. *Makromol. Chem.* **1985**, *186*, 1239–1244.

Hellferich, F. *Ion Exchange*; Dover: New York, 1995.

Inoue, K.; Baba, Y.; Yoshiguza, K. Adsorption of metal ions on chitosan and cross-linked copper(II)-complexed chitosan. *Bull. Chem. Soc. Jpn.* **1993**, *66*, 2915–2921.

Jang, L. K.; Brand, W.; Resong, M.; Maineri, W. Feasability of using alginate to adsorb dissolved copper from aqueous media. *Environ. Prog.* **1990**, *9*, 269–274.

Jha, I. N.; Iyengar, L.; Prabhakara Rao, A. V. S. Removal of cadmium using chitosan. *J. Environ. Eng., ASCE* **1988**, *114*, 962–974.

Kawamura, Y.; Mitsuhashi, M.; Tanibe, H.; Yoshida, H. Adsorption of metal ions on polyaminated highly porous chitosan chelating resin. *Ind. Eng. Chem. Res.* **1993**, *32*, 386–391.

Krajewska, B. Pore structure of chitosan membranes. Capillary pore model. In *Chitin World*; Karnicki, Z. S., Wojtasz-Pajak, A., Brzeski, M. M., Bykowski, P. J., Eds.; Wirtschaftsverlag NW: Bremerhaven, 1995; pp 530–536.

McKay, G.; Poots, V. J. Kinetics and diffusion processes in colour removal from effluent using wood as an adsorbant. *J. Chem. Technol. Biotechnol.* **1980**, *30*, 279–292.

McKay, G.; Otterburn, M. S.; Sweeney, A. G. The removal of colour from effluent using various adsorbents—III. Silica: rate processes. *Water Res.* **1980**, *14*, 15–20.

McKay, G.; Blair, H. S.; Findon, A. Equilibrium studies for the sorption of metal ions onto chitosan. *Indian. J. Chem.* **1989**, *28A*, 356–360.

Michard, P.; Guibal, E.; Vincent, T.; Le Cloirec, P. Sorption and desorption of uranyl ions by silica gel: pH, particle size and porosity effects. *Microporous Mater.* **1996**, *5*, 309–324.

Morris, C. J., Weber, W. J. Advances in water pollution research: Removal of biologically resistant pollutants from wastewaters by adsorption. *Proceedings of the 1st International Conference on Water Pollution Research;* Pergamon Press: New York, 1962; Vol. 2, pp 231–266.

Muzzarelli, R. A. A.; Tanfani, F.; Emanuelli, M.; Bolognini, L. Aspartate glucan, glycine glucan and serine glucan for the removal of cobalt and copper from solutions and brines. *Biotechnol. Bioeng.* **1985**, *27*, 1115–1121.

Nestle, N. F. E. I.; Kimmich, R. Concentration-dependent diffusion coefficients and sorption isotherms. Application to ion exchange processes as an example. *J. Phys. Chem.* **1996**, *100*, 12569–12573.

Papelis, C.; Hayes, K. F.; Leckie, J. O. *HYDRAQL: a program for the computation of chemical equilibrium composition of aqueous batch systems including surface-complexation modeling of ion adsorption at the oxide / solution interface*; Technical Report No. 306; Environmental Engineering & Science, Department of Civil Engineering, Stanford University: Stanford, CA, Sept 1988.

Papelis, C.; Roberts, P. V.; Leckie, J. O. Modeling the rate of cadmium and selenite adsorption on micro- and mesoporous transition aluminas. *Environ. Sci. Technol.* **1995**, *29*, 1099–1108.

Piron, E.; Accominotti, M.; Domard, A. Interaction between chitosan and uranyl ions. role of physical and physicochemical parameters on the kinetics of sorption. *Langmuir* **1997**, *13*, 1653–1658.

Renkin, E. M. Filtration, diffusion and molecular sieving through porous cellulose membranes. *J. Gen. Physiol.* **1954**, *38*, 225–243.

Roberts, G. A. F. *Chitin Chemistry*; MacMillan: London, 1992.

Rorrer, G. L.; Hsien, T. Y.; Way, J. D. Synthesis of porous-magnetic chitosan beads for removal of cadmium ions from wastewater. *Ind. Eng. Chem. Res.* **1993**, *32*, 2170–2178.

Tanaka, H.; Matsumura, M.; Veliky, I. A. Diffusion characteristics of substrates in Ca-alginate gel beads. *Biotechnol. Bioeng.* **1984**, *26*, 53–58.

Tien, C. *Adsorption calculations and modeling*; Series in Chemical Engineering; Butterworth-Heinemann: Boston, 1994.

Tobin, J. M.; Copper, D. G.; Neufeld, R. J. Uptake of metal ions by *Rhizopus arrhizus* biomass. *Appl. Environ. Microbiol.* **1984**, *47*, 821–824.

Vanysek, P. Ionic conductivity and diffusion at infinite dilution. In CRC *Handbook of Chemistry and Physics*, 74th ed.; Linde, D. R., Ed.; CRC: Boca Raton, 1993; 5–90/5–92.

Volesky, B.; Holan, Z. R. Biosorption of heavy metals. *Biotechnol. Prog.* **1995**, *11*, 235–250

Weber, W. J.; DiGiano, F. A. *Process dynamics in environmental systems*; Environmental Science and Technology Series; Wiley & Sons: New York, 1996.